Early Results from the Advanced Radiation Protection Thick GCR Shielding Project

Ryan B. Norman[1], Martha Clowdsley[1], Tony Slaba[1], Lawrence Heilbronn[2], Cary Zeitlin[3], Sean Kenny[1], Luis Crespo[1], Daniel Giesy[1], James Warner[1], Natalie McGirl[2], Luis Castellanos[2], Ashwin Srikrishna[2], Matthew Beach[4], Amir Bahadori[5], Brandon Reddell[6] and Robert Singleterry[1]

[1]NASA Langley Research Center, Hampton, VA 23681, USA (e-mail: ryan.b.norman@nasa.gov)
[2]University of Tennessee, Knoxville, TN 37996, USA
[3]Leidos, Houston, TX 77058, USA
[4]National Institute of Aerospace, Hampton, VA 23681, USA
[5]Kansas State University, Manhattan, KS 66506, USA
[6]NASA Johnson Space Center, Houston, TX 77058, USA

I. Introduction

The Advanced Radiation Protection Thick Galactic Cosmic Ray (GCR) Shielding Project leverages experimental and modeling approaches to validate a predicted minimum in the radiation exposure versus shielding depth curve. Preliminary results of space radiation models indicate that a minimum in the dose equivalent versus aluminum shielding thickness may exist in the 20-30 g/cm^2 region. For greater shield thickness, dose equivalent increases due to secondary neutron and light particle production. This result goes against the long held belief in the space radiation shielding community that increasing shielding thickness will decrease risk to crew health. A comprehensive modeling effort was undertaken to verify the preliminary modeling results using multiple Monte Carlo and deterministic space radiation transport codes. These results verified the preliminary findings of a minimum and helped drive the design of the experimental component of the project. In first-of-their-kind experiments performed at the NASA Space Radiation Laboratory, neutrons and light ions were measured between large thicknesses of aluminum shielding. Both an upstream and a downstream shield were incorporated into the experiment to represent the radiation environment inside a spacecraft. These measurements are used to validate the Monte Carlo codes and derive uncertainty distributions for exposure estimates behind thick shielding similar to that provided by spacecraft on a Mars mission. Preliminary results for all aspects of the project will be presented.

II. Background

Traditionally, space radiation shielding strategy was based on the premise that increasing the total shielding decreased the radiation hazards for astronauts. The assumption was backed by numerous studies using the NASA space radiation transport code HZETRN which confirmed that radiation exposure decreased with increasing shielding, albeit with decreasing effectiveness at larger shielding depths.

As research in space radiation modeling progressed, HZETRN was updated. The early versions of HZETRN [Wilson et al. 1991] assumed all particles traveled in the forward direction along a common axis and in macroscopic shielding materials, such that the loss of particles through production in directions other than straight ahead was balanced by particles produced from parallel neighboring areas entering. Updates to HZETRN introduced methods for handling forward and backward transport along a straight line for neutrons [Slaba et al. 2010]. Additionally, the production and transport of pions, muons, electrons, positrons, and photons (collectively called pion and electromagnetic cascade (π/EM) throughout the text) was added to HZETRN [Norman et al. 2013]. The most recent version of HZETRN, called 3DHZETRN allows for a full three-dimensional treatment for neutrons and light ions (nuclear charge $Z \leq 2$) [Wilson et al. 2014, 2015].

Once HZETRN was updated with π/EM transport and forward-backward treatment for neutrons, dose equivalent as a function of shielding depth was investigated with equal amounts of shielding before and behind the target point to mimic a space habitat. A surprising result was discovered; it is shown in Figure 1. Notice that for the aluminum shield case, when forward-backward neutrons and π/EM are included, the dose equivalent decreases until approximately 40 g/cm^2 of aluminum shielding, after which the dose equivalent begins to increase with increased shielding thickness. This is in contrast to the historical result which is shown as the dotted line in Figure 1. The increase in dose equivalent with increasing shield thickness is largely due to the buildup of neutrons due to the forward-backward neutron transport formalism.

The results for a polyethylene shield are also shown in Figure 1. Due to the high hydrogen content of polyethylene, the neutron buildup is attenuated due to multiple causes including,

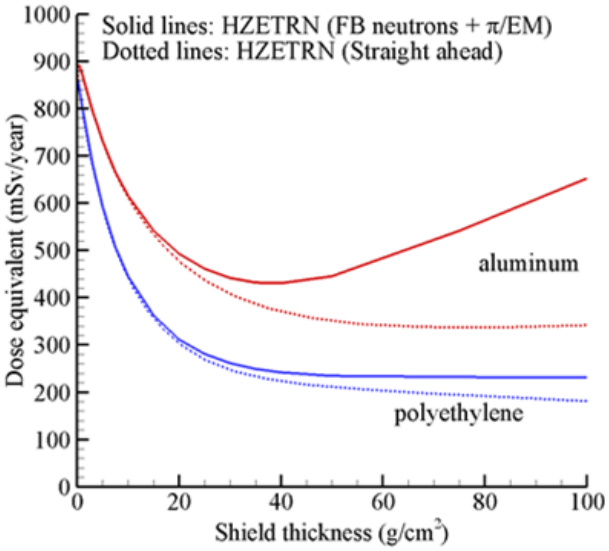

Figure 1. Dose equivalent as a function of shielding thickness as calculated by HZETRN for both aluminum and polyethylene shielding materials.

but not limited to, forward focusing of neutron elastic scattering off hydrogen, increased efficiency of hydrogen to attenuate neutrons, and reduced target fragmentation. Therefore, the dose equivalent flattens out at higher depths instead of increasing.

A local minimum in the radiation exposure versus shielding depth, if found to exist, would be a radical departure from the traditional space radiation shielding design strategy. There would then be an optimum shield thickness that should be designed to minimize the radiation exposure. Vehicle designers would then need to minimize overly thick areas of radiation shielding. Further design complexity would be introduced by the variety of materials acting as a shield (e.g., stored food and water). This motivated the development of a comprehensive strategy to verify the minimum with other radiation transport codes, to validate the minimum using laboratory beam measurements, and to quantify the uncertainty in HZETRN to understand how accurately the exposure minimum is known.

III. Verification

To verify the local minimum in dose equivalent, multiple Monte Carlo space radiation codes were used along with the latest version of 3DHZETRN [Slaba et al., 2017]. The design of the simulations is shown in Figure 2. The lateral dimensions were maximized to ensure there was no leakage out of the shielding volume in the lateral dimension. An equal amount of shielding is located before and after the water target. So, for example, if the front (upstream) target is 5 g/cm^2, the back (downstream) target would also be 5 g/cm^2. The thin water target was set to 0.3 mm and was used to model the tissue response. A thickness of 0.3 mm was found to be large enough to accurately capture energy deposition but not large enough to create spurious nuclear interactions that would alter the results.

For this work, the 1977 solar minimum GCR environment as modeled by the 2010 Badhwar-O'Neill model [O'Neill, 2010] was used. Four Monte Carlo radiation transport codes were used to simulate the transport of the external GCR environment through the shielding environment: FLUKA [Ferrari et al. 2005], Geant4 [Agostinelli et al. 2003], MCNP6 [Goorley 2014], and PHITS [Sato et al. 2013]. Within Geant4, two different nuclear models, Quantum Molecular Dynamics (QMD) and Liege Intranuclear Cascade (INCL), were used and are reported separately. In addition to the Monte Carlo models, 3DHZETRN was also used to investigate the shielding minimum, since the newest version of HZETRN was not used in the original analysis that discovered the possibility of the radiation exposure minimum in shielding. 3DHZETRN can be executed in 1D within the straight-ahead approximation (labeled N=1 throughout the text) or bi-directional transport mode (labeled as N=2 throughout). 3DHZETRN with N=34 denotes that 34 different directions were used to account for the 3D nature of the particle production and transport. Through testing this was found to be sufficient.

Figure 3 shows the results of all models for both aluminum and polyethylene shielding. The most recent results for aluminum shielding (Figure 3, left pane) show that the local minimum in the response has shifted closer to 20 g/cm^2 for all models. Therefore, the validation plan was adjusted to include measurement at 20 g/cm^2. The variation among the 3D models relative to the average (shown as a percent difference in the figure) is small and grows slightly with increasing shielding depth. 3DHZETRN (N=34) results show a less pronounced minimum compared to the Monte Carlo codes, though the position of the minimum is similar. The location of the minimum and variation between models would be suppressed in finite geometry due to particle leakage and would be further suppressed with body self-shielding.

The polyethylene results do not show the increase in dose equivalent with increasing shield thickness due to the superior shielding attributes of the material. Polyethylene has a large hydrogen content and therefore does a better job of attenuating neutrons and protons, thereby minimizing the buildup of light particles in the shielding material at large thicknesses. Overall variation among the models for polyethylene shielding was very similar to that of aluminum shielding.

IV. Validation

To validate the exposure minimum in the thick shielding benchmarks, a comprehensive plan was established for a series of measurements at the NASA Space Radiation Laboratory (NSRL). The plan was developed to best represent the external GCR environment using a set of beams corresponding to important GCR ions at a number of energies. 5 ions (hydrogen, helium, carbon, silicon, and iron) at 3 energies each (400 MeV/nucleon, 800 MeV/nucleon, and 1.5 GeV/nucleon for heavy ions and 2.5 GeV/nucleon for hydrogen) were used for all shielding configurations.

The shielding configuration chosen was a new design never before considered for evaluation in a beam line, with both an upstream and downstream target (both relative to the detectors). Upstream targets are located before the detectors and are directly struck by the beam. Downstream targets are placed after the detectors and are a source of backward directed particles into the

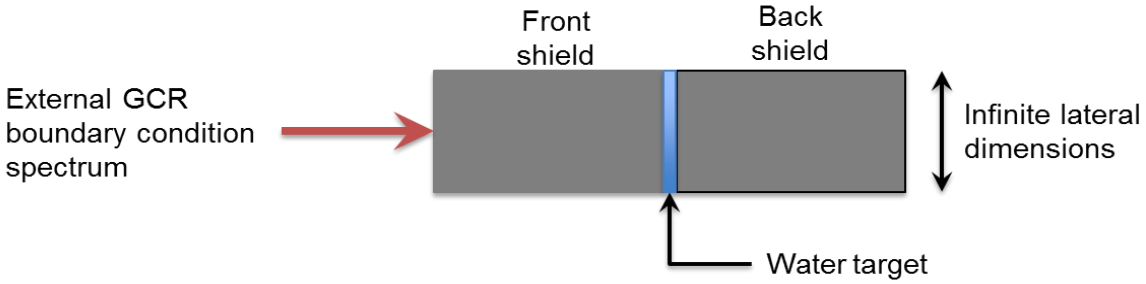

Figure 2. A schematic view of the verification setup used for all models.

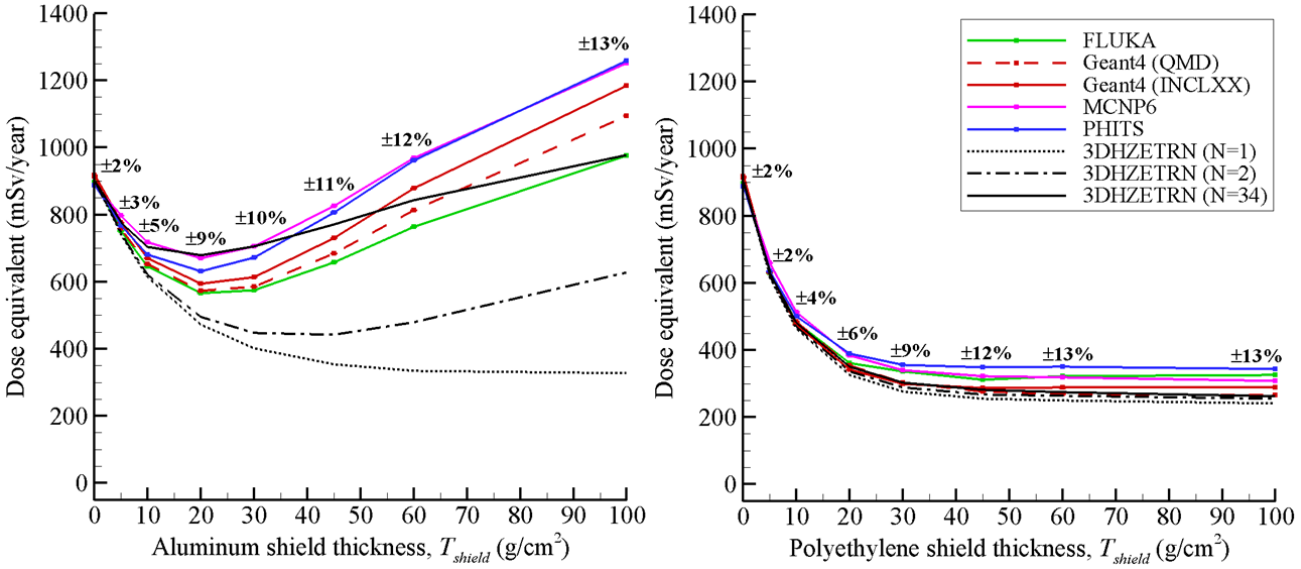

Figure 3. Total dose equivalent for aluminum (left) and polyethylene (right) targets for 1977 solar minimum GCR environment as modeled by multiple transport codes

detector. The upstream target was a varying thickness of aluminum, polyethylene, or aluminum/polyethylene combinations. For a single material, thicknesses of 20, 40, and 60 g/cm^2 were chosen for the upstream target with 60 g/cm^2 downstream target of the same material. For the aluminum/polyethylene combination, either 10 g/cm^2 aluminum followed by (relative to the beam) 10 g/cm^2 polyethylene and 60 g/cm^2 polyethylene downstream or 10 g/cm^2 aluminum followed by 50 g/cm^2 polyethylene upstream with the same 60 g/cm^2 polyethylene downstream target are tested.

Six liquid scintillators were used for both charged particle and neutron detection at 10, 30, 45, 60, 80, and 135 degrees. Two thin, solid plastic scintillators were placed directly in front of each liquid scintillator and were used to separate charged particles from neutral particles. Three arrays of sodium-iodide (NaI) detectors were used for charged particle detection at 0, 10, and 30 degrees, along with nine thin solid plastic scintillators for triggering the NaI detectors. Two thin solid plastic scintillators were used as trigger detectors for event timing and placed before the upstream target.

In March 2016, 100 hours at NSRL were dedicated to the thick target project. Hydrogen beams with energies 400 and 800 MeV, along with 400 MeV/nucleon helium and iron beams, and an iron beam at 800 MeV/nucleon were run with all three upstream aluminum targets. These are shown in blue in Table 1. In November and December of 2016, 200 hours were spent finishing the aluminum targets for all beams and energies and performing measurements with polyethylene targets at all thicknesses for hydrogen, helium, and iron beams at all energies. These measurement combinations are shown in red in Table 1. Another 200 hours of measurement time is scheduled for November and December of 2017 to finish the measurement campaign.

Data analysis is ongoing for the 2016 data runs, with finalized results due later in 2017. Finalized data for the 2017 experiments is expected in 2018.

V. Uncertainty Quantification

In order to reliably extrapolate from uncertainty in laboratory measurements to those in the space environment, uncertainty quantification models must be developed. The strategy used in this project is to first quantify the prediction uncertainty of the Monte Carlo transport models used in the verification phase compared to the experimental measurements. The uncertainty will then be extrapolated to HZETRN results for the full GCR environment.

Table 1. Beam Measurement Test Matrix

Beams (MeV/nucleon)	H			He			C			Si			Fe		
400	Al	CH_2	Al/ CH_2	Al	CH_2	Al/ CH_2	Al	CH_2	Al/ CH_2	Al	CH_2	Al/ CH_2	Al	CH_2	Al/ CH_2
800	Al	CH_2	Al/ CH_2	Al	CH_2	Al/ CH_2	Al	CH_2	Al/ CH_2	Al	CH_2	Al/ CH_2	Al	CH_2	Al/ CH_2
1500 (2500 for H)	Al	CH_2	Al/ CH_2	Al	CH_2	Al/ CH_2	Al	CH_2	Al/ CH_2	Al	CH_2	Al/ CH_2	Al	CH_2	Al/ CH_2

Even with 500 hours of measurements, the experiments only sparsely sample the full GCR spectrum. Therefore, the uncertainty quantification model must be able to use supplemental information, some of which comes from the Monte Carlo comparisons and expert opinion. In addition, balloon measurements at high altitudes in Earth's atmosphere have measured particle flux at energies much larger than those available in the laboratory. These data provide reliable, direct comparison between HZETRN and GCR-produced particle measurements and allow a method to anchor the extrapolation to high energy.

In order to mathematically model the transport code uncertainty compared to the measurements, multiple uncertainty quantification models were investigated [Crespo et al., 2016a]. The three UQ models investigated were Bayesian Inference (BI), Gaussian Process (GP), and Interval Predictor Models (IPMs). The BI and GP models are considered state of the art uncertainty quantification methods used extensively in the literature. IPMs are a newer methodology [Crespo et al., 2016b,c]. The three methods were evaluated on the basis of conservatism, reliability, and computational efficiency compared to a known data generation mechanism defined in Crespo et al. [2016a]. Conservatism is meant in the sense of how tightly or loosely the UQ model bounds the results. An overly conservative UQ model is undesirable as it would inflate the uncertainty in the transport model. Reliability is meant herein to be a probabilistic certification of the correctness of the prediction. Computational efficiency was chosen as a basis for evaluation to balance the effort and computational resources. Since the real answer was known, due to the data generating mechanism being defined, the three UQ models could be compared to the truth in a well-defined way. The IPM methods were found to be the least conservative, yielding the tightest uncertainty bounds, the only model to provide a reliability guarantee, and the most computationally efficient.

IPM methods were then used to compare two of the Monte Carlo simulations to the experimental data. Figure 4 shows an example of an IPM for protons measured at 10 degrees produced from the 800 MeV/nucleon iron beam incident on a 20 g/cm^2 aluminum upstream target. The vertical axis shows the difference between the experimental flux measurements compared to two different flux simulations. The units for the flux are normalized per source particle (SP) per solid angle in units of steradian (ster) per kinetic energy in units of MeV. MCNP is shown in yellow and PHITS is showed in green. The boxes show the simple arithmetic difference between experiment and simulation. The same energy bins were used in the Monte Carlo models as those used in the experimental analysis. The colored lines are the result of the IPM. Results close to zero indicate better agreement for simulation results compared to experiment. At lower energies, MCNP gives results which predict a much larger flux compared to both PHITS and the experiment. Near 100 MeV, the two simulations predict very similar fluxes of protons and then both Monte Carlo models trend very closely at energies above 150 MeV.

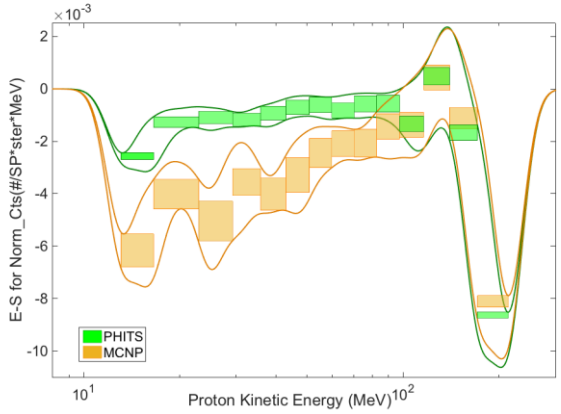

Figure 4. Results of IPM for MCNP (yellow) and PHITS (green) for 800 MeV/nucleon iron beam incident on 20 g/cm^2 aluminum upstream target for protons measured at 10 degrees. Color boxes show actual values for experiment minus simulation and colored lines are the IPM.

The ultimate goal of this component of the project is to quantify the uncertainty in HZETRN for realistic shielding scenarios. The IPMs for beam measurements will be combined with information from the Monte Carlo benchmarks, HZETRN validation with balloon measurements in Earth's upper atmosphere, and expert opinion to create a model of HZETRN response uncertainty in complex vehicles for the full GCR environment.

VI. Conclusions

The Monte Carlo benchmarks verified the existence of the local minimum in dose equivalent as a function thickness in aluminum shielding. 3DHZETRN, along with all Monte Carlo models, found the minimum to occur at smaller thickness nearer to 20 g/cm^2. For polyethylene shielding, the benchmarks showed variation in dose equivalent similar to aluminum, but the minimum is extremely shallow or the dose equivalent simply flattens out after approximately 20 g/cm^2. The variation in dose equivalent between the models was investigated in Slaba et al. (2017) and found to be due to difference in the light ion nuclear physics models. However, all models show the production of nucleons and light ions as the main contributors to the build-up in exposure beyond the minimum.

To validate the existence of the minimum behind thick shielding, laboratory measurements at NSRL were undertaken. 300 hours of measurement time have already been completed with another 200 hours planned for fall 2017. The novel experimental design includes shielding both before and after the detectors, mimicking a space habitat and the verification benchmark studies. Results of the experiments are set to be finalized in 2018.

To quantify the uncertainty in HZETRN for realistic thick shielding, a multifaceted uncertainty quantification effort was devised. The experimental results from the validation component of this project will be used to quantify the uncertainty for the different Monte Carlo models. This will then be used to extrapolate from the Monte Carlo models to HZETRN. The experiments only sparsely cover the GCR environment, and therefore, multiple methods are being used to inform the uncertainty quantification. Specifically, comparison of HZETRN to balloon measurements of light ion flux in the upper atmosphere of Earth will help guide the extrapolation to

high energies that will be important in vehicle and habitat analysis.

ACKNOWLEDGMENT

This work was supported by the Advanced Radiation Protection Project under the Game Changing Division of the Space Technology Mission Directorate of NASA.

REFERENCES

Agostinelli, S. et al., "Geant4 – a simulation toolkit," Nucl. Instrum. Meth. Phys. Res. A, vol. 506, pp.250-303, 2003.

Crespo L. G., S. P. Kenny, and D. Giesy, "A comparative analysis of metamodeling techniques using numerical experiments," AIAA Scitech, Jan 4-8, 2016a.

Crespo L. G., S. P. Kenny, D. Giesy, R. B. Norman, and S. R. Blattnig, "Application of interval predictor models to space radiation shielding," AIAA Scitech, Jan 4-8, 2016b.

Crespo L. G., S. P. Kenny, D. P. Giesy, "Interval predictor models with a linear parameter dependency," J. Verif. Valid. Uncert., vol. 1, pp. 0211007, 2016c.

Ferrari, A., P. R. Sala, A. Fasso, J. Ranft, "FLUKA: a multiparticle transport code," CERN 2005-10 / SLAC-R-773, 2005.

Goorley, T., "MCNP6.1.1-Beta release notes," LA-UR-14-24680, 2014.

Norman, R. B., T. C. Slaba, S. R. Blattnig, "An extension of HZETRN for cosmic ray initiated electromagnetic cascades," Adv. Space Res., vol. 51, pp. 2251-2260, 2013.

O'Neill, P. M., "Badhwas-O'Neill galactic cosmic ray flux model – revised," IEEE Trans. Nuc. Sci., vol. 57, pp. 3148-3153, 2010.

Sato, T. et al., "Particle and heavy ion transport code system PHITS, version 2.52," J. Nucl. Sci. Technol., vol. 50, pp. 913-923, 2013.

Slaba, T. C., S. R. Blattnig, S. K. Aghara, L. W. Townsend, T. Handler, T. A. Gabriel, L. S. Pinsky, B. Reddell, "Coupled neutron transport for HZETRN," Radiat. Meas., vol. 45, pp. 173-182, 2010.

Slaba, T. C., A. A. Bahadori, B. D. Reddell, R. C. Singleterry, M. S. Clowdsley, and S. R. Blattnig, "Optimal shielding thickness for galactic cosmic ray environments," Life Sci. Space Res., vol. 12, pp. 1-15, 2017.

Wilson, J. W., L. W. Townsend, W. Schimmerling, G. S. Khandelwal, F. Khan, J. E. Nealy, F. A. Cucinotta, L. C. Simonsen, J. L. Shinn, J. W. Norbury, "Transport methods and interactions for space radiations," NASA RP 1257, 1991.

Wilson, J. W., T. C. Slaba, F. F. Badavi, B. D. Reddell, A. A. Bahadori, "Advances in NASA radiation transport research: 3DHZETRN," Life Sci. Space Res., vol. 2, pp. 6-22, 2014.

Wilson, J. W., T. C. Slaba, F. F. Badavi, B. D. Reddell, A. A. Bahadori, "3DHZETRN: shielded ICRU spherical phantom," Life Sci. Space Res., vol. 4, pp. 46-61, 2015.